An Efficient and Safe Trans-complementation System for MPXV Mimicking Authentic Viral Infection

Jianying Liu[1,*], Longchao Zhu[1,*], Lingling Mei[1], Yuanyuan Liu[1], Yuanyuan Qu[1], Yulin Yuan[1], Fenfen Zhang[1], Yingyi Cao[2], Yibin Zhu[2], Wanbo Tai[1], Jun Ma[1], Min Zheng[1], Xiaolu Shi[3], Yang Liu[1,#], Gong Cheng[2,3,4,#]

1 Institute of Infectious Diseases, Shenzhen Bay Laboratory, Shenzhen 518000, China.
2 New Cornerstone Science Laboratory, Tsinghua University-Peking University Joint Center for Life Sciences, School of Basic Medical Sciences, Tsinghua University, Beijing 100084, China.
3 Institute of Pathogenic Organisms, Shenzhen Center for Disease Control and Prevention, Shenzhen 518055, China.
4 Southwest United Graduate School, Kunming 650092, China.

* These authors contribute equally.
# Corresponding to liuy@szbl.ac.cn, gongcheng@mail.tsinghua.edu.cn.

Abstract

Since the Mpox virus (MPXV) outbreak in 2022, there have been 97,745 cases and 203 fatalities. This outbreak features increased transmission efficiency and a higher infection rate in the MSM population, with the underlying causes remaining unknown. The requirement of BSL-3 laboratories poses a barrier to MPXV research and antiviral development. Here, we report an efficient and safe trans-complementary system that produces a single-round infectious MPXV, preserving the virus's authentic architecture and enabling it to complete its life cycle in complementing cells. This deficient MPXV genome, lacking two essential genes crucial for late gene transcription and viral assembly, is restricted to a single-round infection in non-complementing cell lines. Notably, SCID mice inoculated with this deficient MPXV exhibited no detectable disease or viral load. This deficient MPXV platform has demonstrated its capacity to study innate immunity and cell death during infection in complementing cells. It can also be used for antibody neutralization assays and anti-MPXV drug evaluation. This trans-complementation platform, safe for use in low-biosafety laboratories, offers a valuable resource for MPXV research and countermeasure development.

Key words: Mpox virus, Reverse genetic, Trans-complementary system, High-throughput drug screening

Introduction

In the first half of 2022, the Mpox virus (formerly monkeypox virus, MPXV) suddenly emerged in multiple countries and rapidly spread. To date, a total of 97,745 laboratory confirmed cases and 660 probable cases, including 203 deaths, have been reported to WHO from 116 countries[1]. The primary natural hosts of the MPXV are mammals such as rodents, and it mainly spreads through close contact. Symptoms of MPXV range from fever, headache, and rash to severe complications like pneumonia and sepsis, potentially leading to death[2]. The MPXV has two primary genetic evolutionary branches: the West African clade with a 1% fatality rate and the Congo Basin clade with a higher fatality rate of up to 10%[3]. Evidence indicates the 2022 MPXV outbreak is genetically linked to the 2017-2018 Nigerian Mpox epidemic, suggesting it originated from the ongoing evolution of that strain[4]. The MPXV genome, composed of double-stranded DNA, typically evolves at a slow pace. However, the 2022 epidemic strain has surpassed the expected mutation rate, indicating an accelerated evolution of the virus[5]. These adapted mutations may alter the infectivity and transmission capabilities of the current epidemic MPXV. The widespread transmission of MPXV among MSM (Men who have Sex with Men) populations also indicate a potential change in tissue and organ preferences[6,7]. However, due to the lack of efficient and safe reverse genetic tools for MPXV, there is no definitive biological evidence to support these claims. The functional and phenotypic changes associated with these mutations, as well as the underlying causes and molecular mechanisms, have not been clearly elucidated.

The MPXV is enveloped, approximately 200-300 nm in diameter, brick-shaped, and features a dumbbell-shaped core[8]. The genome of the MPXV is characterized by a large, double-stranded DNA structure, approximately 197 kilobases in length. The MPXV genome encodes for numerous proteins, involved in various aspects of the virus's life cycle, replication, and interaction with the host's immune system. During the life cycle of the MPXV, two forms of viral particles are present: Intracellular Mature Virus (IMV) and Extracellular Enveloped Virus (EEV). The IMV possesses a single layer of the cellular membrane, whereas the EEV gradually acquires a double-layered phosphatidylethanolamine membrane through a trans-Golgi transport process. Both forms of viral particles are infectious[9]. The Mpox virus infection within cells progresses through early, intermediate, and late stages. Upon entering the cells, both IMV and EEV release prepackaged viral proteins and enzymatic factors into the cytoplasm, stimulating expression of early genes. Early protein synthesis triggers DNA replication,

71 and production of intermediate transcription factors, followed by expression of late
72 genes, mainly structural proteins. Eventually, virions assemble from DNA concatemers,
73 incorporating all the necessary components for initiating a new infection cycle[10].
74 Until now, several infectious clone systems of Orthopoxvirus genus have been
75 established, including vaccinia virus (VACV)[11], horsepox virus (HPXV)[12], cowpox virus
76 (CPXV)[13]. The trans-complementation deficient virus system represents a novel viral
77 platform for the studies of high pathogenic viruses under low biosafety conditions[14].
78 This deficient virus lacks several essential genes necessary for viral replication and
79 propagation, allowing for progeny production of the deficient virus only within specific
80 cell lines that complement these essential genes[14]. To generate the trans-
81 complementation system of MPXV, we selected the G9R and A1L genes on the MPXV,
82 based on the previous research of Orthopoxvirus genus viruses. The G9R gene
83 encodes a late transcription factor VLTF-1, while A1L gene encodes the late
84 transcription factor VLTF-2, both are highly conserved across poxviruses[15]. These two
85 genes have been proven essential for infection and replication within the poxvirus
86 family; loss of either one of them results in the lethality of the poxvirus[16,17]. The
87 locations of these two critical genes, widely separated on the genome, further reduces
88 the risk of viral homologous recombination reverting to the wild type.
89 In our study, we chemically synthesized 56 Mpox viral genome fragments and
90 assembled them into the complete viral genome *in vitro*, omitting two essential genes,
91 G9R and A1L, and incorporating two fluorescence reporters under the intermediate
92 (G9R) and late (A46R) gene promoters. Supported by fowlpox virus (FWPV), the
93 modified MPXV genome with a hairpin structure was transfected into Vero E6
94 G9R+A1L complementing cells to rescue the live virus[11]. We assessed the
95 pathogenicity and stability of this deficient MPXV, confirming its safety in various cell
96 types and SCID mice[18]. Notably, the deficient MPXV was shown to elicit standard
97 immune responses and cell death in complementing cell lines. Additionally, the
98 integrated reporter genes proved useful for antibody neutralization tests and high-
99 throughput drug screening. Our results indicate that this MPXV trans-complementation
100 system is safe for low-biosafety conditions, providing a significant tool for MPXV basic
101 and applied research.

Results

A trans-complementary deficient MPXV system

The trans-complementation system for MPXV produces deficient viral particles capable of only a single round of infection in non-complementing cells[14]. This system includes: (1) viral genomic DNA without the essential G9R and A1L late transcription factors, crucial for viral vitality, and (2) a complementing cell line that continuously expresses the G9R and A1L proteins. The 197 kb MPXV genomic DNA from the MA001 strain (ON563414.3) was segmented into 56 smaller fragments, chemically synthesized individually. These fragments were then assembled into seven larger fragments and inserted into the pSMART plasmid for amplification. Subsequently, these seven fragments were digested using Type II restriction enzymes and ligated to construct the complete MPXV genome *in vitro*. This deficient viral genome omits two essential genes, G9R and A1L, and features a mNeonGreen fluorescence gene at the beginning of the non-essential A46R gene, linked via a 2A linker, alongside a mCherry fluorescence gene under the G9R gene promoter (termed as MPXV G9R+A1L-KO) (Fig. 1a). Successful ligation of the seven large fragments was confirmed by PCR targeting the discontinuous regions between each of these fragments (Extended Data Fig. 1a). The hairpin structure, essential for Orthopoxviruses, was chemically synthesized and its structure integrity was verified with Mung bean nuclease treatment (Extended Data Fig. 1b). Hairpins were ligated to both ends of the viral genome to generate a functional genomic DNA construct, as confirmed by Sanger sequencing across the ligation site.

To produce complementing cells, the G9R and A1L genes (linked by IRES,internal ribosomal entry site) were incorporated into a lentivirus delivery system, which included puromycin or blasticidin for antibiotic selection. The Vero E6 (African green monkey kidney) cells were infected with recombinant lentivirus and after a two-week antibiotic selection, isolated Vero E6 G9R+A1L colonies were analyzed by western blot and immunofluorescence assay (IFA) to verify the expression of G9R and A1L genes (Fig. 1b,c). The Vero E6 G9R+A1L stable cell lines were then pre-infected with FWPV two hours prior to transfection with the deficient MPXV G9R+A1L-KO genome. FWPV facilitated the initiation of early-stage RNA transcription in the deficient MPXV, a process shared among all Orthopoxviruses. Due to species-specific constraints, the FWPV failed to produce infectious viral particles in mammalian cells. Therefore, only the progeny of the deficient MPXV was reproduced after several days of incubation

136 (Fig. 1d). Typically, significant cytopathic effects (CPE) are noticeable 5 to 7 days after
137 transfection (Fig. 1e). The cells are then harvested 10 days post-transfection, at which
138 point significant cell death is observed in about half of the cell population. The deficient
139 MPXV G9R+A1L-KO forms plaques in the Vero E6 G9R+A1L cells normally (Fig. 1f)[19]
140 and can effectively amplify in the complementing cells (Fig. 1g and Extended Data Fig.
141 2a), simultaneously generating a green fluorescence signal (Fig. 1h). Then, the
142 deficient viral particles were purified through sucrose density gradient centrifugation
143 and analyzed using western blot with an anti-MPXV A35R polyclonal antibody
144 (Extended Data Fig. 2b). The negative staining of MPXV G9R+A1L-KO particles by a
145 transmission electron microscope confirmed their structural integrity (Fig. 1i). To further
146 verify the integrity of the viral genome, genomic DNA of MPXV G9R+A1L-KO was
147 isolated from the aliquoted viral stock and digested with selected restriction enzymes.
148 The resulting DNA fragments were then characterized by pulsed-field gel
149 electrophoresis (Fig. 1j). These results demonstrate that the deficient MPXV
150 G9R+A1L-KO was successfully rescued and efficiently reproduced in complementing
151 cells, with a normal poxvirus structure and an intact full-length genome. Sequencing
152 results indicate that the final rescued Mpox virus has two synonymous mutations in the
153 coding region (A75900T and T182846A) and an 18 bp deletion in the non-coding
154 region (179205-179222); otherwise, the sequence is completely accurate.
155
156 **The deficient MPXV exhibited sing-round infection in non-complementing cells**
157 The MPXV G9R+A1L-KO virus, lacking two essential genes for viral reproduction,
158 was restricted to single-round infections in non-complementing cells. It regains its
159 reproductive capacity and produces progeny viruses only when infecting cells that fully
160 complemented both G9R and A1L genes (Fig. 2a). To determine the lethality linked to
161 these two genes, the MPXV G9R+A1L-KO was infected in cells partially
162 complementing either the G9R or A1L gene (Fig. 2b). Notably, MPXV-G9R+A1L-KO
163 failed to replicate in cells complementing only one gene and did not produce any green
164 fluorescence four days post-infection (Fig. 2c,d). Subsequently, 14 non-
165 complementing cell lines from various mammals, including animals and humans, and
166 each derived from different tissues, were selected to assess the replication ability of
167 MPXV G9R+A1L-KO. These cell lines were inoculated with a high initial multiplicity of
168 infection (MOI) of 1 (Fig. 2e, f). Supernatants with cell lysates were collected daily for
169 plaque assays. For the first two days, a small residual of the inoculated virus was

170 detected, but no amplification occurred in any non-complementing cell line from day 3
171 to day 5 (Fig. 2e). The fluorescence detection clearly showed the absence of green
172 fluorescence in non-complementing cells from day 1 to day 5, while the deficient virus
173 replicated efficiently in the Vero E6 G9R+A1L complementing cells (Fig. 2f, Extended
174 Data Fig. 3).
175
176 **The deficient MPXV was reproducible in various complementing cell lines**
177 Vero E6 cells are immune-deficient and lack the capability to produce interferon.
178 Given this, we investigated whether MPXV G9R+A1L-KO could amplify in other
179 G9R+A1L complementing immune-competent cell lines. Using the G9R+A1L lentiviral
180 system, we introduced these two complementary genes into 8 representative cell lines.
181 Following antibiotic selection, we assessed the expression of these two knocked-in
182 genes by western blot. Blotting results confirmed the successful expression of the G9R
183 and A1L genes in 8 cell lines, although expression levels varied among the different
184 cells (Extended Data Fig. 4). Upon inoculating these stable cell lines with MPXV
185 G9R+A1L KO, the virus rapidly amplified in all of them. The amplification showed
186 significant variation, with the highest viral load observed in 22RV1 cells, derived from
187 human prostate carcinoma epithelial cells (Fig. 2g). This result indicated that the MPXV
188 MA001 strain may have a tissue preference for prostate carcinoma epithelial, which
189 may correlate with the increased infection rates in MSM populations during this
190 outbreak[6]. It should be noted that no correlation was observed between the viral load
191 and the expression levels of complementary genes in the cells (Fig. 2g and Extended
192 Data Fig. 4).
193
194 **The deficient MPXV remains stable throughout serial passages**
195 To validate the genetic stability of these deficient viruses, we subcultured MPXV
196 G9R+A1L-KO up to 20 passages (P20) on Vero E6 G9R+A1L cells in three
197 independent replicates. Viruses from P5, P10, P15, and P20 were subjected to PCR
198 analysis to verify the continuous absence of the targeted G9R and A1L genes and the
199 stability of the mNeonGreen fluorescence gene (Extended Data Fig. 5a). All gene
200 deletions and insertions remained stable after 20 passages (Extended Data Fig. 5b).
201 Although the morphology of the plaques appeared slightly larger after 20 passages
202 (Extended Data Fig. 5c), there were no significant green fluorescence changes four
203 days post-infection between P1 and P20 viruses (Extended Data Fig. 5d). Only one

204 mutation (Δ146999T) affecting protein characteristics were consistently detected
205 across three replicates through full genome sequencing (Extended Data Table 1).
206 Additionally, the genomic DNA of deficient MPXV could not be detected by qPCR in
207 non-complementing cells after two blind passages (P2).
208
209 **Safety evaluation of deficient MPXV virions *in vivo***
210 To further evaluate the safety of deficient MPXV *in vivo*, we selected the SCID mice,
211 which were susceptible to Orthopoxvirus infection. We inoculated these mice
212 intraperitoneally with a maximum dose of purified MPXV G9R+A1L-KO virions,
213 equivalent to approximately 10^6 PFU/mouse. An initial titer of 2×10^5 PFU/mouse of
214 vaccinia virus (VACV, tiantan strain) was served as the positive control. Clinical
215 symptoms and body weight were monitored, and blood were collected daily for viral
216 load detection. All mice were sacrificed 9 days post-infection to analyze organ viral
217 loads (Fig. 3a). The results indicated no weight change between the MPXV G9R+A1L-
218 KO and Mock groups, compared to a notable weight loss in VACV-infected mice (Fig.
219 3b). Additionally, no viremia or clinical symptoms were observed in either the Mock or
220 deficient MPXV groups (Fig. 3c,d). Nine days post-infection, no viral nucleotide
221 residuals were detected in organs from the deficient MPXV group, while significant
222 amounts of VACV were present in all organs (Fig. 3e). Pathological analysis revealed
223 clear damage in the lungs and spleens of VACV-infected mice, but not in those from
224 the deficient MPXV and Mock groups (Fig. 3f). These results demonstrate that deficient
225 MPXV G9R+A1L-KO induces only a single-round infection and lacks virulence in mice.
226
227 **The deficient MPXV regulates the innate immune response**
228 The deficient MPXV retains the ability to modulate immune responses and activate
229 other cellular signaling pathways, including programmed cell death, in complementing
230 cell lines. MPXV G9R+A1L-KO was introduced at an MOI of 0.1 into IFN-α stimulated
231 Hela G9R+A1L cells, with the RNA transcriptome measured at 48 hours post-infection.
232 Results indicated that while IFN-α significantly upregulated interferon-stimulated
233 genes (ISGs), MPXV showed a robust inhibitory effect on ISG expression (Fig. 4a),
234 demonstrating similar transcriptome profiles to those in VACV-infected cells[20].
235 Meanwhile, like typical Orthopoxvirus infections, inoculation of MPXV G9R+A1L-KO in
236 Hela G9R+A1L cells induced slow but apparent cell death over time, with nearly 20%
237 of cells dying at 48 hours post-infection (Fig. 4b,c). The activation of apoptosis was

238 indicated by the cleavage of caspase 3, 7, and 8 in deficient MPXV-infected cells (Fig.
239 4d). These results suggest that this trans-complementation system is a valuable
240 platform for studying innate immune and inflammatory responses, as well as cell death,
241 during MPXV infection *in vitro*.
242
243 **The anti-MPXV antibodies and drugs evaluation by deficient MPXV**
244 Due to the extensive capacity of the MPXV genome, the deficient MPXV system can
245 accommodate multiple reporters, including fluorescence proteins and luciferase etc.
246 This allows for the establishment of a high-throughput system for screening and
247 evaluating anti-MPXV antibodies and drugs. Firstly, we compared the antibody
248 neutralization capabilities of two previously reported mAbs, 8AH8AI[21] and 7D11[22],
249 against MPXV G9R+A1L-KO and VACV using the $PRNT_{50}$ assay, the gold standard
250 for antibody neutralization tests. These two antibodies neutralized MPXV G9R+A1L-
251 KO as effectively as VACV, demonstrating that viral particles produced by the trans-
252 complementation system are suitable for assessing antibody efficacy (Fig. 4e,f).
253 Subsequently, we evaluated the potential of the deficient MPXV for high-throughput
254 drug screening (Fig. 4g). MPXV G9R+A1L-KO was pre-mixed with various drugs
255 previously reported to have anti-MPXV capabilities[23-25]. The anti-MPXV IC_{50} values for
256 these compounds were then determined using the classical plaque-forming unit (PFU)
257 assay and a high-throughput green fluorescence cell counting method, respectively.
258 Notably, two drugs, tecovirimat and cidofovir, displayed potent anti-MPXV efficacy (Fig.
259 4h,i). The IC_{50} values measured by our trans-complementation system were consistent
260 with those reported in previous studies using authentic live virus[23,24]. Furthermore, we
261 compared the correlation of IC_{50} values derived from the PFU and fluorescence
262 methods, finding that the results from both methods were comparable and correlated
263 well (Fig. 4j, Extended Data Table 2). These findings suggest that this MPXV trans-
264 complementation system is effective for high-throughput, automated screening and
265 evaluation of antibodies and drugs.

266 **Discussion**

267 Our reverse genetic trans-complementation platform for MPXV, along with various
268 complementing cells, offers a powerful tool for *in vitro* studies on MPXV genetic
269 evolution, life cycle, as well as the induced innate immune responses and programmed
270 cell death. The assembly of the full-length deficient MPXV can be achieved by T4
271 ligation of seven individual fragments *in vitro*, offering several advantages over
272 traditional recombination and single plaque selection methods[11]. This *in vitro* approach
273 provides an alternative method for obtaining genetically modified MPXV, avoiding the
274 complex plasmid transfer processes across yeast and bacteria. Additionally, multiple
275 mutations or genetic modifications can be simultaneously introduced into the MPXV
276 genome, eliminating the need for multiple rounds of single virus plaque screening and
277 identification. It may also reduce the frequency of unexpected mutations and
278 recombination compared to the *in vivo* assembly system[12].

279 The primary advantage of this deficient MPXV system is its enhanced safety. For
280 high-pathogenicity viruses, direct genetic modification of the wild-type virus could
281 potentially enhance pathogenicity, raising biosafety and bioethical concerns. The
282 trans-complementation system introduces an additional safety lock for reverse genetic
283 engineering. The conditional replication in complementing cells confines the modified
284 pathogens to these specific cells, significantly reducing risks to operators and the
285 environment. Our results indicate that immune regulation and programmed cell death
286 function normally in complementing cells with deficient MPXV, maintaining the capacity
287 for MPXV-host interaction studies. Moreover, the viral structure is identical to the
288 authentic virus, ensuring the system's efficacy for antibody and drug screening while
289 maintaining safety (Fig. 4).

290 Fowlpox virus was employed to trigger the initiate transcription of the MPXV
291 G9R+A1L-KO DNA genome due to the conservation of polymerases with the
292 Orthopoxvirus genus. Once entry into the cells, FWPV releases its RNA polymerase
293 from the virion core, which then recognizes and initiates transcription and replication
294 of the deficient MPXV genome. However, due to the absence and variation of specific
295 accessory proteins, FWPV fails to assemble in mammalian cells and does not produce
296 progeny viruses. his strategy ensures that only pure deficient MPXV particles are
297 assembled and released, eliminating the need for single viral plaque selection and
298 reducing the time required for mutant virus rescue. In cells infected with the produced
299 deficient MPXV virus, the residual fowlpox virus genome was no longer detectable by

qPCR.

In our trans-complementation system, we integrated two fluorescent proteins into the deficient MPXV genome. The mCherry gene, replacing the absent G9R gene, is regulated by intermediate transcription factors. The mNeonGreen gene was fused to the beginning of the late-expressed A46R gene. As a result, even without complementation of G9R and A1L genes, a high initial MOI infection of deficient MPXV in non-complementing cells can trigger red fluorescence, while green fluorescence appears only in cells where successful complementation occurs. Therefore, the red fluorescence can serve as a tool to evaluate viral single-round entry and replication, providing a quick and effective assessment approach in primary cells lacking complementation.

The Mpox virus genome does not enter the cell nucleus, resulting in a very low probability of recombining with the host cell genome. However, this trans-complementation system, while reducing safety concerns, still presents some risks due to MPXV's double-stranded DNA nature, which could potentially recombine with other spontaneously infected poxviruses. To further minimize recombination risks, the two excised essential genes are broadly separated on the MPXV genome, and the complementary genes are codon optimized with different flanking nucleotide sequences. This spacing reduces the chance of reverting to a fully functional wild-type MPXV through a single recombination event. It should be noted that, although recombination between deficient MPXV and complementing genes in cells is unlikely, there is still a possibility that deficient MPXV could undergo long-segment recombination with other poxviruses to produce “chimeric viruses”. To mitigate this risk, co-infection of deficient MPXV with other mammalian poxviruses should be avoided. On the other hand, we tested complementing systems lacking three or more essential genes; however, they showed reduced reproductive efficiency. The two-gene knockout system represents the optimal compromise between safety and efficiency. Crucially, our extensive *in vitro* and *in vivo* safety evaluations affirm the adequacy of this two-gene knockout strategy.

Utilizing this trans-complementation deficient MPXV system, we can investigate specific MPXV gene functions by knocking out or modifying them, including introducing single amino acid mutations to pinpoint those critical for the 2022 MPXV epidemic. Concurrently, we can study crucial host genes influencing MPXV infection and reproduction using a CRISPR-Cas9 single-gene knockout library in complementing

334 cells. Additionally, we can fuse fluorescent proteins to various non-essential MPXV
335 genes to label different regions of the viral particle, such as the extra-membrane, intra-
336 membrane, and core, allowing for precise tracking of cell attachment, entry, and
337 movement via single-particle microscopy. Furthermore, we can generate custom-
338 engineered viral tools for anti-MPXV antibody and drug screening and evaluation.
339 Overall, our study offers a comprehensive platform for studying MPXV infection,
340 deciphering disease progression, and developing countermeasures under low-safety
341 conditions.

342 **Methods**

343 **Ethics statement**

344 Mouse studies were performed in accordance with the guidance for the Care and Use
345 of Laboratory Animals of the Shenzhen Bay Laboratory (SZBL). The protocol was
346 approved by the Institutional Animal Care and Use Committee (IACUC) at SZBL. All
347 the animal operations were performed under anesthesia by isoflurane to minimize
348 animal suffering.

349 **Animals and cells**

350 CB17-SCID female mice were purchased from Syagen Biotechnology company
351 (Suzhou, China). Vero E6 (CL-0491), Caco-2 (CL-0050), 22RV1 (CL-0004), RK-13
352 (CL-0501), LLC-MK2 (CL-0141), SW-13 (CL-0451A), DU 145 (CL-0075), A549 (CL-
353 0016), 293T (CL-0005), Hela (CL-0101), OVCAR-3 (CL-0178), JEG-3 (CL-0127),
354 HCT-8 (CL-0098), HTR-8 (CL-0765) cells were purchased from Procell (Wuhan, China)
355 and cultured in high-glucose Dulbecco's modified Eagle's medium (DMEM,
356 C11965500BT, Gibco) supplemented with 2 mM L-glutamine, 100 U/mL Penicillin-
357 Streptomycin (P/S, 15140122, Gibco), and 10% fetal bovine serum (FBS; HyClone
358 Laboratories, UT). For G9R+A1L complementing cell lines, the following
359 concentrations of puromycin (ant-pr-1, InvivoGen) or blasticidin (ant-bl-1, InvivoGen)
360 were supplemented respectively: Vero E6 G9R+A1L (puromycin, 1:500), RK13
361 G9R+A1L (puromycin, 1:4000), 22RV1 G9R+A1L (puromycin, 1:2000), Caco-2
362 G9R+A1L (puromycin, 1:1000), OVCAR-3 G9R+A1L (puromycin, 1:2000), A549
363 G9R+A1L (blasticidin, 1:100), DU 145 G9R+A1L (puromycin, 1:5000), 293T G9R+A1L
364 (blasticidin, 1:200), and Hela G9R+A1L (blasticidin, 1:2000). All other culture media
365 and supplements were purchased from ThermoFisher Scientific. All cell lines were
366 authenticated using STR methods and tested negative for mycoplasma.

367 **Construction of the MPXV deficient infectious clone**

368 For the construction of the deficient MPXV G9R+A1L-KO infectious virus, 56 DNA
369 fragments covering the full-length MPXV genome (MA001 strain) were chemically
370 synthesized by Qingke company. The deletions of the G9R and A1L genes, along with
371 the insertion of fluorescent proteins, were introduced into the respective regions of
372 genome (Fig. 1a). To generate the F1 to F7 sub-genomic fragments, seven to eight
373 small DNA fragments were assembled the pSMART-BAC 2.0 (42030, Lucigen) plasmid

backbone using Gibson Assembly (E2621L, NEB). These recombinant plasmids were then introduced into BAC-Optimized Replicator v2.0 electrocompetent cells (60210, Lucigen) via electroporation at 2500V, 25μF, 300Ω using the Bio-Rad GenePluser Xcell Total system (1652660, Bio-Rad). To construct the full-length MPXV G9R+A1L KO genome, the F1 to F7 plasmids were digested with the PaqCI enzyme (R0745L, NEB) and assembled *in vitro* using T4 ligase (M0202M, NEB) along with hairpins at both ends. The hairpins were chemically synthesized by Qingke company. The hairpin ssDNA sequence is 5'-CACATTTTTTTCTAGACACTAAATAAAATAGTAAAATATAATATTAATGTACTAAAACTTATGTATTATTAATTTATCTAACTAAAGTTAGTAAATTATATACATAATTTTATAATTAATTTAATTTTACTATTTTATTTAGTGTCTAGAAAAAAA-3'. The successful ligation of fragments was verified by PCR across the ligation sites and DNA sequencing. The ligation products were then introduced into Vero E6 G9R+A1L complementing cells to rescue the virus. The primers used for MPXV construction was listed in Extended Data Table 3.

Selection of G9R+A1L complementing cell lines

To construct cell lines expressing the MPXV G9R+A1L proteins, the Flag-G9R and HA-A1L genes were chemically synthesized and optimized for mammalian codon expression. For packaging the lentivirus, the pLVX-G9R+A1L-puromycin or pLVX-G9R+A1L-blasticidin plasmids were transfected into 293T cells using the Lenti-X Packaging Single Shots kit (631275, TaKaRa). Lentiviral supernatants were harvested 48 hours post-transfection and filtered through a 0.45 μm membrane (SLHV033RB, Millipore, Burlington, MA). One day before transduction, target cells were seeded in a 6-well plate with DMEM containing 10% FBS. After 12-18 hours, cells were transduced with 0.5 mL of lentivirus for 24 hours in the presence of 12 μg/mL of polybrene (107689, Sigma-Aldrich, St. Louis, MO). Twenty-four hours after transduction, cells from a single well were distributed into four 10-cm dishes and cultured in medium supplemented with the designated concentration of puromycin or blasticidin. The medium containing antibiotics was refreshed every 2 days. After 2-3 weeks of selection, visible puromycin or blasticidin-resistant cell colonies were formed. Select colonies were moved into 24-well plates. Upon reaching confluence, cells were treated with trypsin and replated in 6-well plates for further growth. These cells were designated as P0 cells. For cell line validation, total cellular mRNA was extracted, subjected to RT-PCR, followed by cDNA sequencing of the G9R and A1L genes, and protein expression was verified via

408 western blot.

409 **Rescue of the deficient MPXV G9R+A1L-KO infectious virus**

410 The deficient MPXV G9R+A1L-KO infectious virus was recovered in the Vero E6
411 G9R+A1L cell line, which constitutively expresses G9R and A1L proteins. In brief,
412 confluent monolayers of the Vero E6 G9R+A1L cell line in 12-well plates were infected
413 with 1 MOI of avian pox virus (Quail adapted strain, CVCC AV1003) for 2 hours prior
414 to MPXV DNA transfection. Subsequently, the culture media were replaced with Opti-
415 MEM (31985062, Gibco), and DNA transfection was performed using Fugene 6
416 reagent (E2691, Promega). 1 μg of MPXV DNA was mixed with 3 μl of Fugene 6
417 reagent 100 μl Opti-MEM medium for 15 minutes at room temperature. The DNA mix
418 was then slowly dripped onto the cells and gently mixed. Post 24-hour incubation, the
419 cell supernatant was replaced with fresh 2% FBS DMEM for continued cultivation. Cell
420 monitoring continued for 8-10 days until the appearance of cytopathic effects (CPE)
421 and expression of mCherry and mNeonGreen fluorescent proteins. The supernatant
422 and cells underwent 2 freezing and thawing cycles at −80 °C. After centrifugation at
423 1000 g for 10 minutes, the supernatants were aliquoted and stored at −80 °C as the
424 P0 virus stock.

425 **Virus plaque assay**

426 10-fold dilutions of the deficient MPXV virus stock were prepared in a 96-well plate in
427 triplicate. The diluted MPXV viruses were added to the Vero E6 G9R+A1L cells for a
428 2-hour incubation. Cells were then washed thrice with DPBS to eliminate any
429 unattached virus particles. 3 mL of overlay medium (2% FBS DMEM with 2% HEPES,
430 1% penicillin/streptomycin, and 0.8% carboxymethyl cellulose) was added over the
431 cells for a 6-day incubation. Subsequently, cells were fixed with 4% formaldehyde for
432 1 hour and stained with 300 μL of 0.5% crystal violet solution for 5 minutes. Plaques
433 were manually counted under whiteboard illumination.

434 **Virus replication kinetics determination**

435 Virus replication kinetics were determined by using a plaque assay as described above.
436 Typically, cell lines were seeded in 24-well plates and cultured at 37 °C with 5% CO_2
437 for 16 hours. Deficient MPXV was then inoculated into the cells at the specified MOI
438 and incubated at 37 °C for 2 hours. Post-infection, cells were washed thrice with DPBS
439 to eliminate any unattached virus particles. At designated time points, supernatants

440 and cells were collected and underwent 2 freezing and thawing cycles. Following
441 centrifugation at 1000 g for 5 minutes, the supernatants were employed to determine
442 virus titers via plaque assay.

443 **The extraction of MPXV genome**

444 For virus DNA extraction, 5 mL of viral culture supernatant was treated with TURBO™
445 DNase (ThermoFisher, AM2238) for 30 minutes at 37°C, followed by RNase A (Sangon
446 Biotech, B600473) for 30 minutes at 37°C. EDTA was then added, and the mixture was
447 incubated at 65°C for 10 minutes to inactivate the DNase. The sample was mixed with
448 virion lysis buffer (2 mg/mL Proteinase K, 6% sodium dodecyl sulfate, 250 mM Tris-
449 HCl, pH 8.0, 20 mM EDTA, pH 8.0) and incubated at 37°C for 2 hours. The MPXV
450 genome was gently extracted using the phenol-chloroform method and precipitated in
451 three volumes of ethanol. Finally, the precipitate was collected by centrifugation at
452 15,000g at 4°C, rinsed with 70% ethanol, briefly dried, and resuspended in 20 μL of
453 ddH_2O.

454 **The pulse-field gel electrophoresis (PFGE)**

455 For pulse-field gel electrophoresis (PFGE), full-length viral genomic DNA was digested
456 with *Pac*I or *Stu*I for 2 hours at 37°C and separated using 1% Seakem Gold agarose
457 gels (Lonza, 50150) prepared with half-strength Tris-borate-EDTA electrophoresis
458 buffer. The DNA fragments were separated by the CHEF Mapper® XA system (BioRad)
459 in Auto Algorithm mode (Molecular Weight: Low, set to 1 kb; Molecular Weight: High,
460 set to 197 kb) for 9 hours at 14°C, using a switching time gradient of 1 to 10 seconds
461 at 6.0 V/cm, a linear ramping factor, and a 120° angle. The DNAs were then visualized
462 with SYBR Gold stain (ThermoFisher, S11494) and imaged using the ChemiDoc MP
463 Imaging System (BioRad).

464 **Virus passage**

465 The confluent monolayers of the Vero E6 G9R+A1L cell line in 6-well plates were
466 infected with 0.1 MOI of deficient MPXV G9R+A1L-KO infectious virus with triple
467 biological replicate. For 2-3 days, supernatants and cells were collected and
468 underwent 2 freezing and thawing cycles. Following centrifugation at 1000 g for 5
469 minutes, the supernatants were aliquoted and stored at −80 °C as the P1A, P1B, P1C
470 virus stock, respectively. 100μl of virus stock was transferred to 100% confluency of
471 the virus producer cell line in the 6 well-plates for propagation. Whole genomic DNA

472 sequencing was performed at every 5 passages by Nanopore sequencing. P0 and P20
473 sequences have been deposited to figshare website (Licence ID: CC BY 4.0, DOI:
474 10.6084/m9.figshare.26340355).
475

476 **Safety evaluation of deficient MPXV in mice model**

477 Three-to-four-week-old female CB17-SCID mice were randomly assigned and
478 intraperitoneally inoculated with 1×10^6 PFU of MPXV-G9R-A1L-KO, 2×10^5 PFU of
479 VACV, or PBS mock control. Throughout the study, the mice were monitored daily for
480 clinical signs. Blood samples were taken daily for viral DNA extraction to detect the
481 presence of the virus. At 10 d.p.i., the mice were euthanized, and tissue samples were
482 collected for hematoxylin and eosin (H&E) staining and virus titration. All samples were
483 then stored at −80 °C until analysis.

484 **Real-time qPCR assay**

485 Deficient MPXV was isolated using the EZNA SE Viral DNA/RNA kit (R6871, Omega)
486 according to the manufacturer's instructions. The absolute copy number of MPXV DNA
487 was quantified using the 2×EasyTaq® PCR SuperMix (AS111-01, TransGene) by Taq-
488 man qPCR. The detection probe and primers were based on the conserved DNA
489 polymerase (F8L) gene and described as follows: Forward primer (5'-TCA ACT GAA
490 AAG GCC ATC TAT G-3'), Reverse primer (5'-GAG TAT AGA GCA CTA TTT CTA AAT
491 CCC A-3'), and probe 5'-FAM-CCA TGC AAT A(T–BHQ1) A CGT ACA AGA TAGTAG
492 CCA AC-Phos-3', both were chemically synthesized by Qingke company. The qPCR
493 reactions were performed using the CFX96 real-time PCR detection system (1855195,
494 Bio-Rad).

495 **Immunofluorescence assay and western blot**

496 For immunofluorescence assay (IFA) staining, Vero E6 G9R+A1L cells were cultured
497 on a Nunc™ Lab-Tek™ II Chamber Slide™ System. G9R and A1L proteins were
498 labeled with primary anti-Flag (F1804, Sigma-Aldrich) and anti-HA (26183, Invitrogen),
499 followed by secondary Alexa Fluor 488 anti-mouse HRP antibody (A28175, Invitrogen).
500 The nuclei were then stained with DAPI. Fluorescence signals were captured using a
501 Nikon fluorescence microscope. For western blot analysis, various types of cells
502 transduced with G9R, A1L, G9R+A1L, or those infected with deficient MPXV were
503 harvested and lysed using RIPA buffer. They were then probed with anti-Flag, anti-HA,

504 and anti-MPXV A35R (RVV13101, AtaGenix) antibodies. The results were analyzed
505 using ImageLab software version 6.0.1 (#12012931, Bio-Rad).

506 **Deficient MPXV antiviral drug evaluation**

507 Vero E6 G9R+A1L cells were seeded in 12-well plates at a specified density. Twenty-
508 four hours post-seeding, MPXV G9R+A1L-KO (with a final inoculation of 50 PFU per
509 well) was pre-mixed with varying drug concentrations before adding to the cells. After
510 a 2-hour incubation at 37°C and 5% CO_2 with gentle rocking every 15 minutes, the
511 inoculum was removed. Cells were then overlaid with a mixture of 2% HEPES, 1%
512 penicillin/streptomycin, and 0.8% carboxymethyl cellulose (C104979, Aladdin) in
513 DMEM, with each condition tested in triplicate. Plates were then incubated for 6 to 8
514 days at 37°C in a 5% CO_2 incubator. Monolayers were fixed in 4% formaldehyde and
515 stained with 0.5% crystal violet. Plaques were manually counted under whiteboard
516 illumination. IC_{50} values were calculated using GraphPad Prism 9.

517 **Deficient MPXV neutralization assay**

518 The neutralizing activity of monoclonal antibodies (mAbs) was determined using the
519 EEV or IMV forms of VACV, or MPXV G9R+A1L-KO in a plaque reduction
520 neutralization (PRNT) assay. Briefly, 100 PFU of either VACV or deficient MPXV were
521 incubated with serial two-fold dilutions of the mAb for 30 minutes at 37°C and then
522 added to monolayers of Vero E6 or Vero E6 G9R+A1L cells in 6-well plates. After a
523 one-hour incubation, cells were overlaid with 0.8% carboxymethyl cellulose in DMEM
524 with 2% FBS and incubated for 3 days (for VACV) or 6 days (for MPXV G9R+A1L-KO)
525 at 37°C in 5% CO_2 to allow plaque formation. Monolayers were then fixed with 4%
526 formaldehyde and stained with 0.5% crystal violet. Plaques were manually counted
527 under whiteboard illumination.

528 **Statistics**

529 Mice were randomly allocated into different groups. The investigators were not blinded
530 to allocation during the experiments or to the outcome assessment. No statistical
531 methods were used to predetermine sample size. Descriptive statistics are provided in
532 the figure legends. A linear regression model in the software Prism 9 (GraphPad) was
533 used to calculate the IC_{50} values from the antiviral assay. Differences between
534 continuous variables were assessed using the non-parametric Mann-Whitney test. The
535 weight loss data are presented as mean ± standard deviation and were statistically

536 analyzed using two-factor analysis of variance (ANOVA) with Tukey's post hoc test. *,
537 $p < 0.05$; **, $p < 0.01$; ***, $p < 0.001$; ****, $p < 0.0001$; ns, $p > 0.05$, not significant.

538 **Data availability**

539 Extended Data includes 5 figures, and 3 tables can be found with this article. Any other
540 information is available upon request. Mpox sequences have been deposited to
541 figshare website (Licence ID: CC BY 4.0, DOI: 10.6084/m9.figshare.26340355).

542 **Acknowledgments**

543 This study was supported by grants from the National Key Research and Development
544 Plan of China (2023YFC2307400, 2021YFC2300200, 2021YFC2302405,
545 2022YFC2303200, 2022YFC2303400, and 2023YFC2305900), the National Natural
546 Science Foundation of China (82241082, 32270182, 82372254, 32188101, 32273099,
547 82271872, 82341046 and 32100755), Shenzhen Medical Research Fund (B2301009),
548 Shenzhen San-Ming Project for Prevention and Research on Vector-borne Diseases
549 (SZSM202211023), Yunnan Provincial Science and Technology Project at Southwest
550 United Graduate School (202302AO370010)，the New Cornerstone Science
551 Foundation through the New Cornerstone Investigator Program, and the Xplorer Prize
552 from Tencent Foundatio n.

553 **Author contributions**

554 G.C., Y.L. and J.L. conceived and designed the study. G.C., Y.L., J.L. and L.Z. wrote
555 and revised the manuscript. J.L., L.Z., L.M., Y.L., Y.Q., Y.Y., F.Z., Y.C., Y.Z., W.T., J.M.,
556 M.Z., X.S. and Y.L. performed the experiments and analyzed the data. All the authors
557 reviewed, critiqued, and provided comments on the text.

558 **Competing financial interests**

559 The authors declare no competing interests.

560 **References**

561 1. WHO. 2022 Monkeypox Outbreak: Global Trends.
562 https://worldhealthorg.shinyapps.io/mpx_global/

563 2. Gong Q, Wang C, Chuai X, Chiu S. Monkeypox virus: a re-emergent threat to
564 humans. *Virol Sin* 2022, 37(4): 477-482.

565 3. Adnan N, Haq ZU, Malik A, Mehmood A, Ishaq U, Faraz M, et al. Human
566 monkeypox virus: An updated review. *Medicine (Baltimore)* 2022, 101(35): e30406.

567 4. Yinka-Ogunleye A, Aruna O, Dalhat M, Ogoina D, McCollum A, Disu Y, et al.
568 Outbreak of human monkeypox in Nigeria in 2017-18: a clinical and
569 epidemiological report. *Lancet Infect Dis* 2019, 19(8): 872-879.

570 5. Isidro J, Borges V, Pinto M, Sobral D, Santos JD, Nunes A, et al. Phylogenomic
571 characterization and signs of microevolution in the 2022 multi-country outbreak of
572 monkeypox virus. *Nat Med* 2022, 28(8): 1569-1572.

573 6. Endo A, Murayama H, Abbott S, Ratnayake R, Pearson CAB, Edmunds WJ, et al.
574 Heavy-tailed sexual contact networks and monkeypox epidemiology in the global
575 outbreak, 2022. *Science* 2022, 378(6615): 90-94.

576 7. O'Toole A, Neher RA, Ndodo N, Borges V, Gannon B, Gomes JP, et al. APOBEC3
577 deaminase editing in mpox virus as evidence for sustained human transmission
578 since at least 2016. *Science* 2023, 382(6670): 595-600.

579 8. Cho CT, Wenner HA. Monkeypox virus. *Bacteriol Rev* 1973, 37(1): 1-18.

580 9. Schmelz M, Sodeik B, Ericsson M, Wolffe EJ, Shida H, Hiller G, et al. Assembly of
581 vaccinia virus: the second wrapping cisterna is derived from the trans Golgi
582 network. *J Virol* 1994, 68(1): 130-147.

583 10. Rubins KH, Hensley LE, Bell GW, Wang C, Lefkowitz EJ, Brown PO, et al.
584 Comparative analysis of viral gene expression programs during poxvirus infection:
585 a transcriptional map of the vaccinia and monkeypox genomes. *PLoS One* 2008,
586 3(7): e2628.

587 11. Domi, A. and B. Moss, Cloning the vaccinia virus genome as a bacterial artificial
588 chromosome in Escherichia coli and recovery of infectious virus in mammalian
589 cells. *Proc Natl Acad Sci U S A* 2002, 99(19): p. 12415-20.

590 12. Noyce RS, Lederman S, Evans DH. Construction of an infectious horsepox virus
591 vaccine from chemically synthesized DNA fragments. *PLoS One* 2018, 13(1):
592 e0188453.

593 13. Roth SJ, Hoper D, Beer M, Feineis S, Tischer BK, Osterrieder N. Recovery of

infectious virus from full-length cowpox virus (CPXV) DNA cloned as a bacterial artificial chromosome (BAC). *Vet Res* 2011, 42(1): 3.

14. Zhang X, Liu Y, Liu J, Bailey AL, Plante KS, Plante JA, et al. A trans-complementation system for SARS-CoV-2 recapitulates authentic viral replication without virulence. *Cell* 2021, 184(8): 2229-2238. e2213.

15. Upton, C., et al., Poxvirus orthologous clusters: toward defining the minimum essential poxvirus genome. *J Virol* 2003. 77(13): p. 7590-600.

16. Zhang Y, Keck JG, Moss B. Transcription of viral late genes is dependent on expression of the viral intermediate gene G8R in cells infected with an inducible conditional-lethal mutant vaccinia virus. *J Virol* 1992, 66(11): 6470-6479.

17. Sutter, G., et al., Stable expression of the vaccinia virus K1L gene in rabbit cells complements the host range defect of a vaccinia virus mutant. *J Virol* 1994, 68(7): p. 4109-16.

18. Futami, M., et al., Efficacy and Safety of Doubly-Regulated Vaccinia Virus in a Mouse Xenograft Model of Multiple Myeloma. *Mol Ther Oncolytics* 2017. 6: p. 57-68.

19. Huang B, Zhao H, Song J, Zhao L, Deng Y, Wang W, et al. Isolation and Characterization of Monkeypox Virus from the First Case of Monkeypox - Chongqing Municipality, China, 2022. *China CDC Wkly* 2022, 4(46): 1019-1024.

20. Hernaez, B., et al., RNA-Seq Based Transcriptome Analysis of the Type I Interferon Host Response upon Vaccinia Virus Infection of Mouse Cells. *J Immunol Res* 2017. 2017: p. 5157626.

21. Chen, Z., et al., Chimpanzee/human mAbs to vaccinia virus B5 protein neutralize vaccinia and smallpox viruses and protect mice against vaccinia virus. *Proc Natl Acad Sci U S A* 2006. 103(6): p. 1882-7.

22. Esqueda, A., et al., A Monoclonal Antibody Produced in Glycoengineered Plants Potently Neutralizes Monkeypox Virus. *Vaccines (Basel)* 2023. 11(7).

23. Warner, B.M., et al., In vitro and in vivo efficacy of tecovirimat against a recently emerged 2022 monkeypox virus isolate. *Sci Transl Med* 2022. 14(673): p. eade7646.

24. Frenois-Veyrat G, Gallardo F, Gorge O, Marcheteau E, Ferraris O, Baidaliuk A, et al. Tecovirimat is effective against human monkeypox virus in vitro at nanomolar concentrations. *Nat Microbiol* 2022, 7(12): 1951-1955.

25. Chiem, K., et al., Identification of In Vitro Inhibitors of Monkeypox Replication. *Microbiol Spectr* 2023. 11(4): p. e0474522.

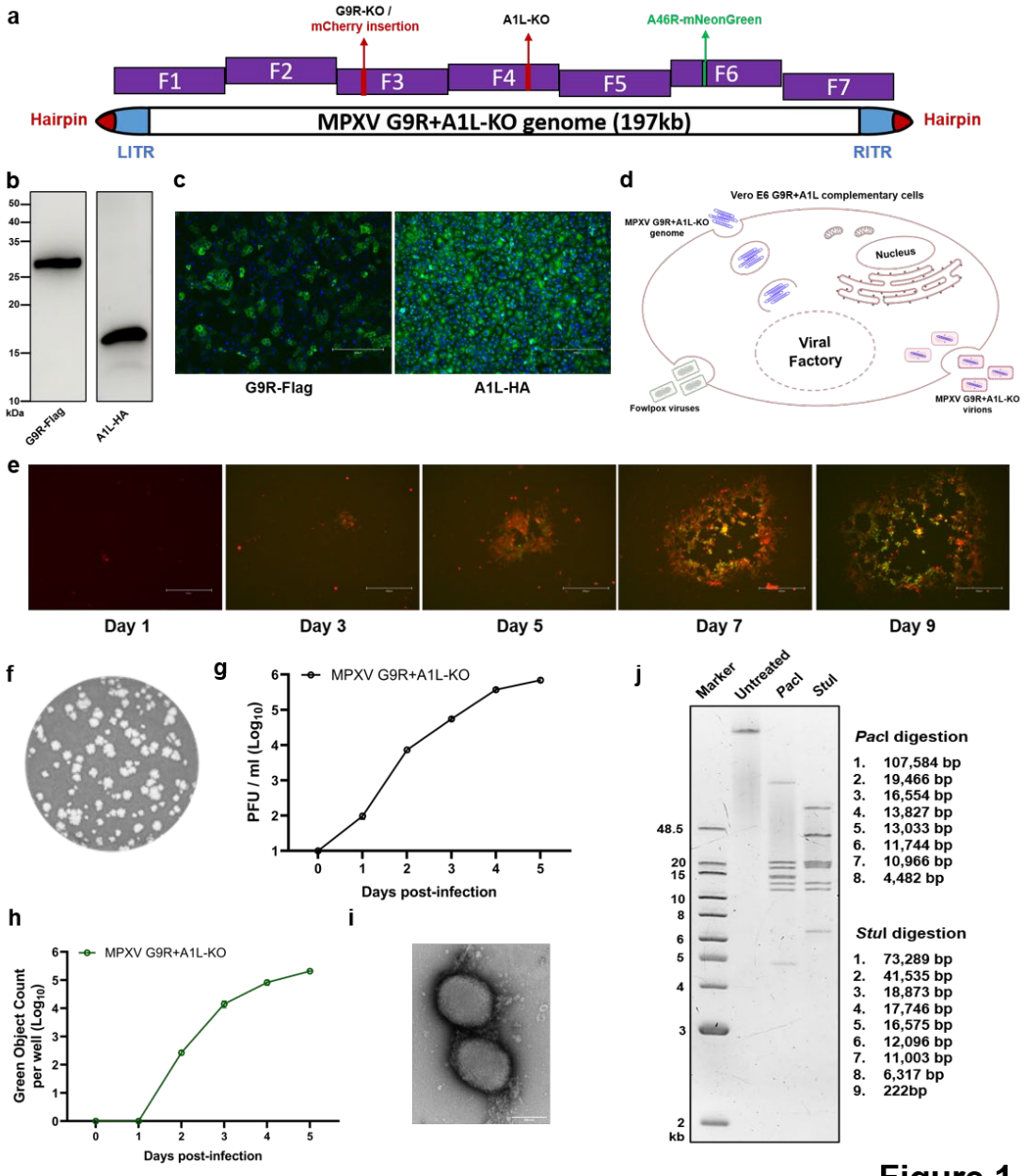

Figure 1. Construction and rescue of trans-complementation deficient Mpox virus.

a, Schematic representation of deficient MPXV G9R+A1L-KO construction. Deletions of the G9R and A1L genes, along with the insertion of fluorescent proteins, were introduced into the backbone of MPXV MA001 strain. The complete MPXV genome was assembled from seven big fragments. Red arrows highlight the loci of G9R and A1L gene knockouts on the MPXV genome, with an mCherry reporter inserted at the G9R site. The green arrow marks the insertion site of the mNeonGreen reporter. **b,c,** The expression and localization of G9R and A1L genes in Vero E6 G9R+A1L complementing cells were detected by western blot **(b)**, and immunofluorescence assay **(c)**; Scale bar, 300 μm. **d,** The diagram for rescue of deficient MPXV infectious clone. The Vero E6 G9R+A1L stable cell lines were pre-infected with FWPV two hours

642 prior to transfection with the deficient MPXV G9R+A1L-KO genome. FWPV facilitated
643 the initiation of early-stage RNA transcription in the deficient MPXV. Due to species-
644 specific constraints, the FWPV failed to produce infectious viral particles in mammalian
645 cells. Therefore, only the progeny of the deficient MPXV was reproduced after several
646 days of incubation. **e,** Observation of time-lapse MPXV G9R+A1L-KO viral plaque
647 formation using mCherry and mNeonGreen fluorescence detection; Scale bar, 300 μm.
648 **f,** Plaque morphology of MPXV G9R+A1L-KO virus in Vero E6 G9R+A1L
649 complementing cells. The experiment was conducted using a plaque assay. Briefly,
650 after a 2-hour incubation with MPXV G9R+A1L-KO virus, the cells were washed with
651 DPBS to remove unattached particles. An overlay medium containing carboxymethyl
652 cellulose was added, and the cells were incubated for 6 days. Plaques were stained
653 with crystal violet. **g,h,** Replication kinetics of MPXV G9R+A1L-KO virus in Vero E6
654 G9R+A1L complementing cells. 0.01 MOI of MPXV G9R+A1L-KO virus was inoculated
655 onto Vero E6 G9R+A1L cells. Following a 2-hour incubation, the cells were washed
656 three times with DPBS and continuously cultured for 5 days with fresh 2% FBS DMEM.
657 The virus titers and mNG-positive cells were determined using a plaque assay (**g**) and
658 fluorescence determination (**h**). **i,** Electron microscopy of MPXV G9R+A1L-KO virus
659 particles with negative staining; Scale bar, 200 nm. **j,** The full-length genomic DNA or
660 restriction enzyme-digested fragments of deficient MPXV were analyzed by pulse-field
661 gel electrophoresis (PFGE). The expected sizes of the digested fragments were
662 presented but fragments smaller than 2 kb will not be detected in this assay.
663

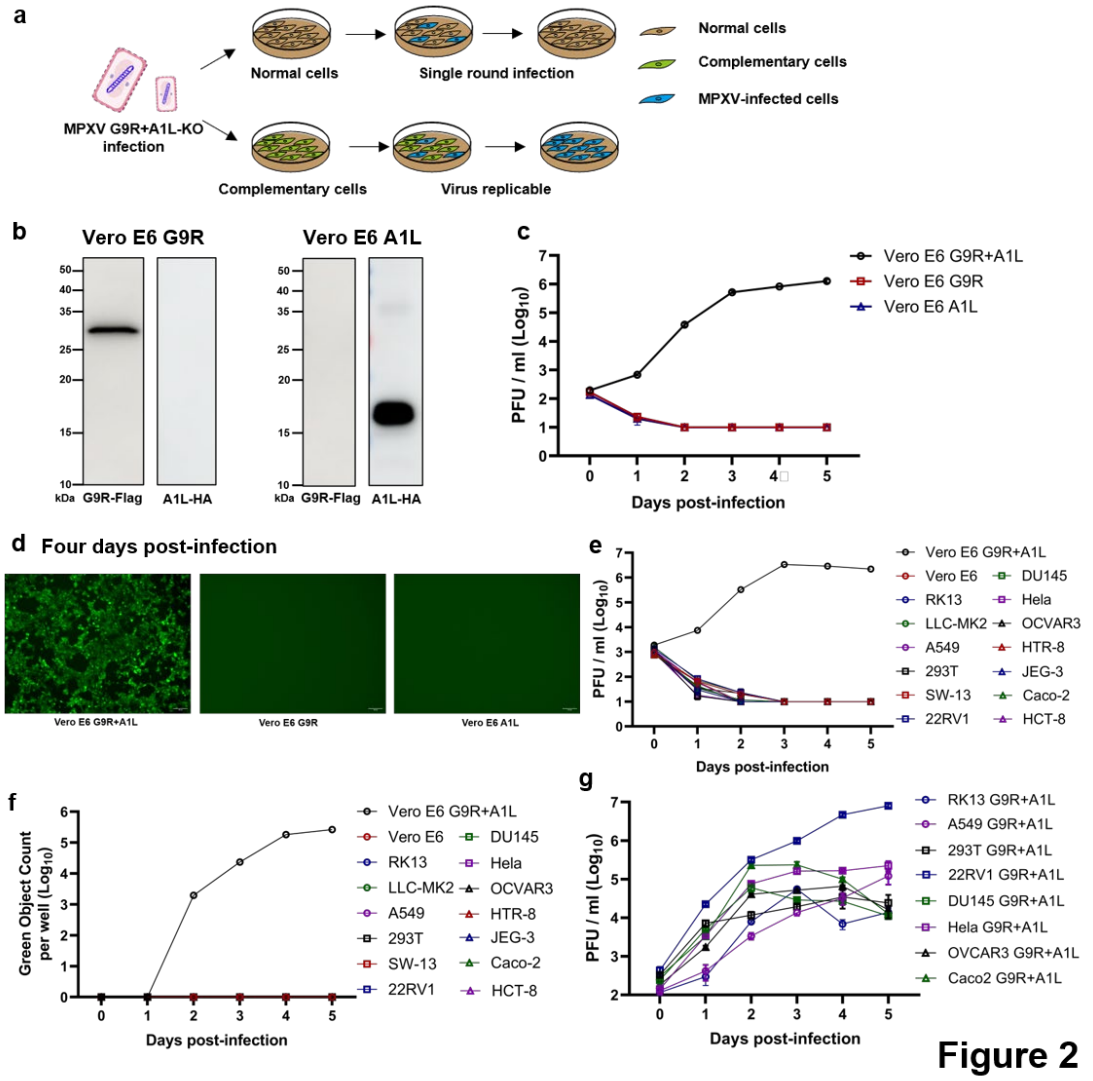

Figure 2. Replication dynamics of MPXV G9R+A1L-KO virion in non-complementing and complementing cells.

a, Schematic representation of the replication of MPXV G9R+A1L-KO virion in both non-complementing and complementing cells. **b,** The expression of G9R and A1L genes in Vero E6 G9R and Vero E6 A1L partially complementing cells respectively. **c,** Replication kinetics of the MPXV G9R+A1L-KO virus in Vero E6 G9R+A1L, Vero E6 G9R, and Vero E6 A1L complementing cells. Each cell type was inoculated with 0.1 MOI of the MPXV G9R+A1L-KO virus. The virus titers were determined using a plaque assay. **d,** Fluorescence microscopy analysis of deficient MPXV infected complementing cell lines. Representative mNeonGreen (mNG) positive images at 4 days post infection are shown. Scale bar, 100 μm. **e,f,** Assessment of single-round infection of MPXV G9R+A1L-KO virus on non-complementing cell lines. 1 MOI of MPXV G9R+A1L-KO virus was inoculated onto 14 different cell lines. The Vero E6 G9R+A1L cell served as positive control. The virus titers and mNG-positive cells were determined using a plaque assay (**e**) and fluorescence determination (**f**). **g,** Replication kinetics of MPXV G9R+A1L-KO virus in different G9R+A1L complementing cells. 0.1 MOI of MPXV G9R+A1L-KO virus was inoculated onto eight G9R+A1L complementing

682 cells. The virus titers were determined using a plaque assay. **c-g,** For different types
683 of cells, the initial number of infected cells is normalized to an equal amount. **c,e,g,**
684 The cells were lysed with the culture medium by freezing and thawing twice for plaque
685 determination at the indicated times. The detection limit for the plaque assay is 10
686 PFU/ml.

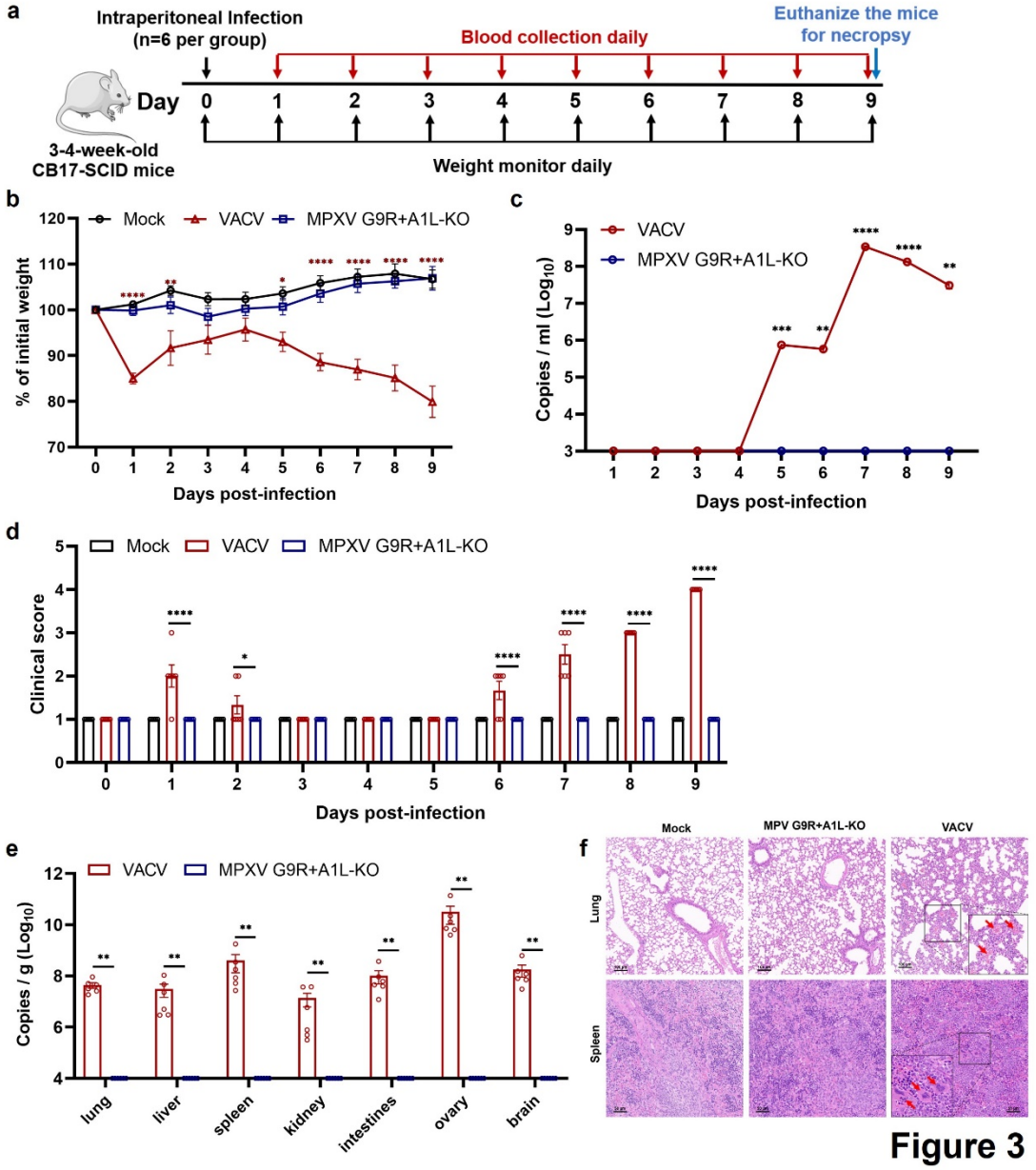

Figure 3. The safety evaluation of MPXV G9R+A1L-KO virion in animal models. **a,** Experimental scheme of MPXV G9R+A1L-KO virus challenge. 3-4 weeks old SCID mice were intraperitoneally (I.P.) inoculated with 1×10^6 PFU of MPXV G9R+A1L-KO virus, 2×10^5 PFU of VACV, or PBS mock control, respectively. Mice were monitored for weight loss, disease, and viral load. **b,** The weight changes of animals after intraperitoneal infection of MPXV G9R+A1L-KO virus (n=6) and VACV (n=6). The uninfected mock group (n=6) served as a negative control. Body weights were recorded daily for 9 days. Data are presented as mean ± standard deviation. Weight changes between MPXV G9R+A1L-KO and mock or VACV groups were assessed using two-way ANOVA with Tukey's post hoc test. The red asterisk indicates a statistical difference between the mock and VACV groups. No significant difference was observed between mock and MPXV G9R+A1L-KO groups. **c,** Viral replication kinetics in serum of infected animals. The amounts of genomic DNA were quantified

701 by quantitative PCR. **d,** Disease of MPXV G9R+A1L-KO and VACV-infected animals.
702 The diseases include ruffled fur, lethargic, hunched posture, and orbital tightening. The
703 clinical scores are presented. P values were adjusted using the Bonferroni correction
704 to account for multiple comparisons. **e,** The viral loads in lung, liver, spleen, kidney,
705 intestines, ovary and brain after infection with G9R+A1L-KO virus and VACV. Dots
706 represent individual animals (n=6). **f,** Pathological observations of lung and spleen
707 sections in mice. Representative hematoxylin and eosin (H&E) staining images were
708 presented. **c-e,** The mean ± standard error of mean is presented. A non-parametric
709 two-tailed Mann-Whitney test was used to determine the differences between VACV
710 and MPXV G9R+A1L-KO groups. **b-e,** Differences were considered significant if $p <$
711 0.05; *, $p < 0.05$; **, $p < 0.01$; ***, $p < 0.001$; ****, $p < 0.0001$.

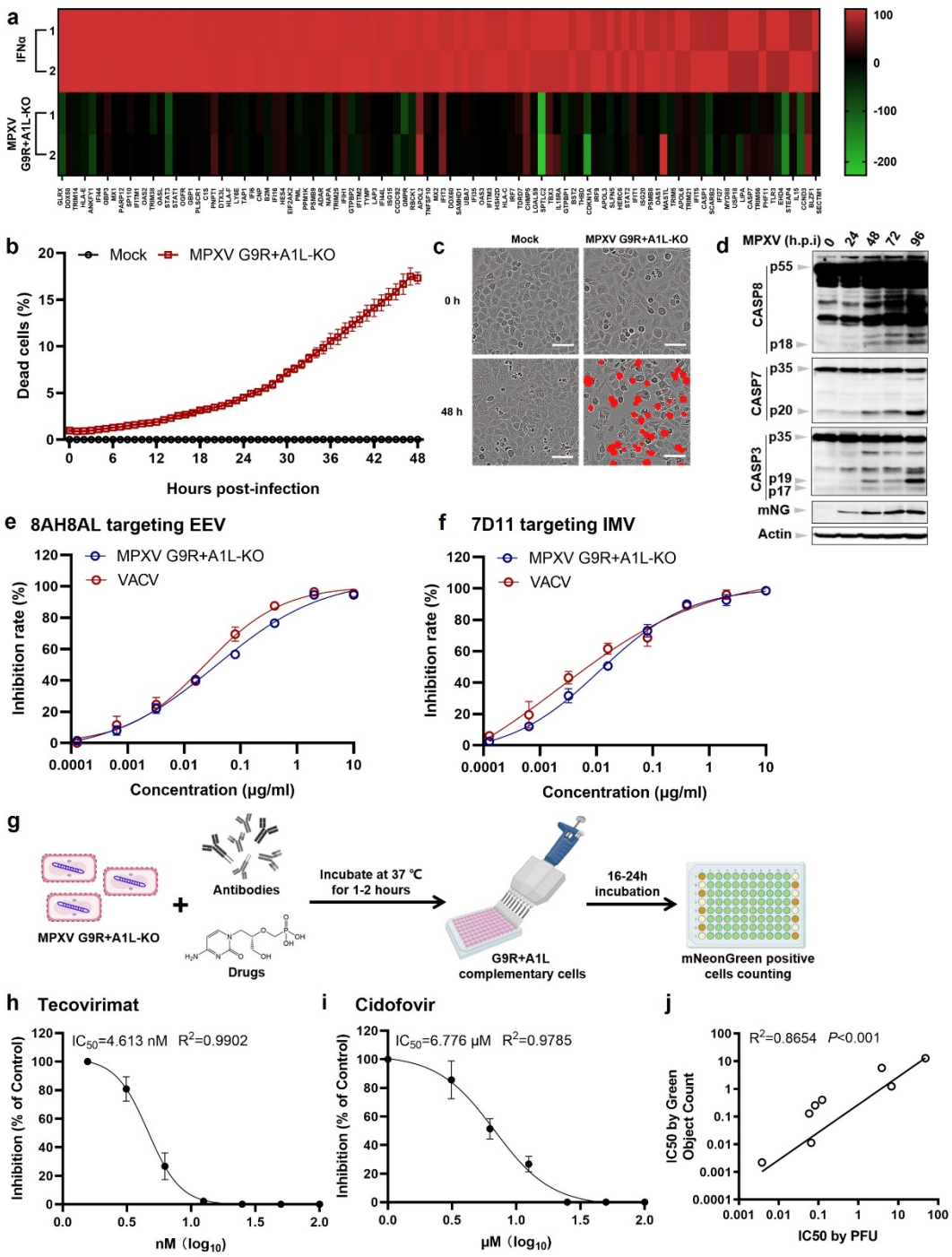

Figure 4

Figure 4. The potential of deficient MPXV for pathogenesis studies, antibody neutralization and high-throughput drug screening.

a, Heatmap of differentially expressed genes (DEGs) associated with IFNα responses in Hela G9R+A1L cells. The heatmap shows the relative percentages of DEGs involved in IFNα responses in deficient MPXV-infected samples versus uninfected cells, with a color scale on the right indicating expression levels. **b-d,** The deficient MPXV stimulates the programmed cell death. **b,** Cell death kinetics were assessed using the IncuCyte live-cell automated system. Hela G9R+A1L cells, seeded in 24-well plates,

721 were infected with MPXV G9R+A1L-KO virus at an MOI of 0.1. Dead cells, stained
722 with propidium iodide (PI), were counted hourly over a 48-hour period. **c,** PI-positive
723 cells were marked with a red mask for visualization. Scale bar, 80 μm. **d,** The activation
724 of caspase 3, 7, and 8 post-MPXV G9R+A1L-KO infection at different time points. **e,f,**
725 Neutralization activity of monoclonal antibodies (mAbs) against MPXV G9R+A1L-KO
726 and VACV. The 8AH8AL(**e**) and 7D11(**f**) antibodies were incubated with EEV and IMV
727 forms of MPXV G9R+A1L-KO and VACV, respectively, for neutralization via a plaque
728 assay. Curves were fitted using nonlinear regression and mean ± standard deviations
729 from two independent experiments were shown. The experiment was conducted twice
730 with similar results. **g,** Scheme diagram for high-throughput MPXV antibody or drug
731 screening using an mNG positive cell counting assay. **h,i,** The IC_{50} assessment of
732 tecovirimat and cidofovir potency against deficient MPXV in complementing cells. Vero
733 E6 G9R+A1L cells were infected with MPXV G9R+A1L-KO virus and treated with
734 indicated concentrations of tecovirimat (**h**) or cidofovir (**i**) for 6 days. Plaque formation
735 inhibition is expressed in %, normalized over control conditions. IC_{50} and R^2 are
736 indicated. Data are presented as mean ± standard deviations. Experiments were
737 performed twice in triplicate. **j,** Correlation analysis of IC_{50} values between the mNG
738 positive cell counting assay and plaque formation assay. The Pearson correlation
739 coefficient (R^2) and p-values (two-tailed) are indicated.
740

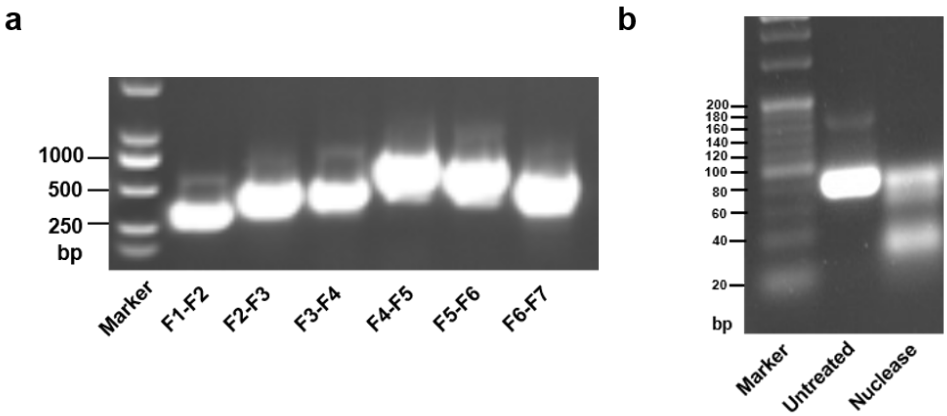

Extended Data Figure 1

Extended Data Figure 1. The validation of the integrity of the full-length MPXV genome and hairpin structures.

a, Validation the integrity of full-length MPXV genome by PCR. Primers spanning fragment junctions were employed to verify the complete assembly of the MPXV genome. **b,** Validation of the secondary structure formation of chemically synthesized MPXV hairpin oligos. The Mung bean exo/endonuclease recognized and digested double strand DNAs.

750

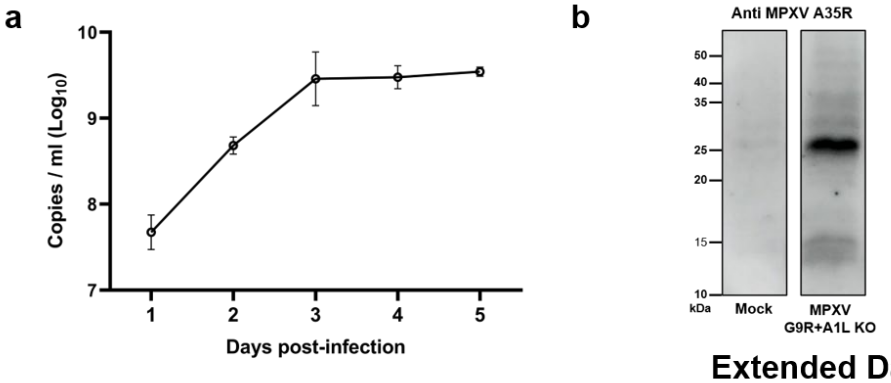

Extended Data Figure 2

751

752 **Extended Data Figure 2. The qPCR and western blot verification of deficient**
753 **MPXV.**
754 **a,** Viral replication kinetics of MPXV G9R+A1L-KO in Vero E6 G9R+A1L cells. The
755 amounts of genomic DNA were quantified by quantitative real-time PCR. **b,** The
756 expression of A35R gene in MPXV G9R+A1L-KO infected or un-infected cell lysates
757 was detected by western blot.

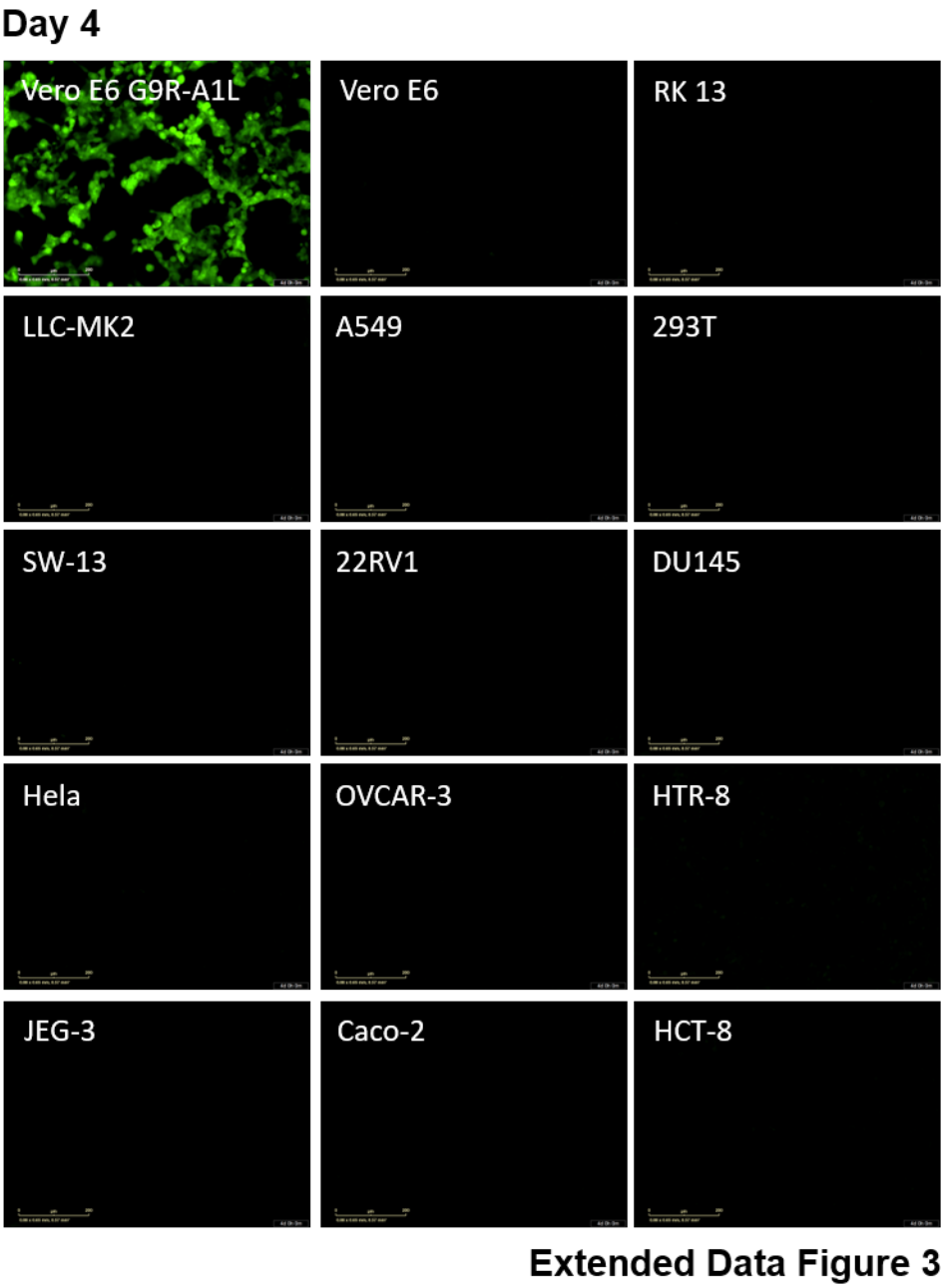

Extended Figure 3. Analysis of deficient MPXV-infected non-complementing and complementing cell lines using fluorescence microscopy.

1 MOI of MPXV G9R+A1L-KO virus was inoculated onto 14 non-complementing cell lines. The Vero E6 G9R+A1L cell was served as a positive control. Representative mNeonGreen positive images at 4 days post infection are shown. Scale bar, 200 μm. Vero E6, African green monkey kidney cells; RK-13, rabbit kidney cells; LLC-MK2, rhesus kidney cells; A549, human non-small cell lung cancer cells; 293T, human embryonic kidney cells; SW-13, human adrenocortical small cell carcinoma cells; 22RV1, human prostate cancer cells; DU 145, human prostate cancer cells; Hela, human cervical cancer cells; OVCAR-3, human ovarian cancer cells; HTR-8, human chorionic trophoblast cells; JEG-3, human chorionic carcinoma cells; Caco-2, human colorectal adenocarcinoma cells; HCT-8, human ileocecal cancer cells.

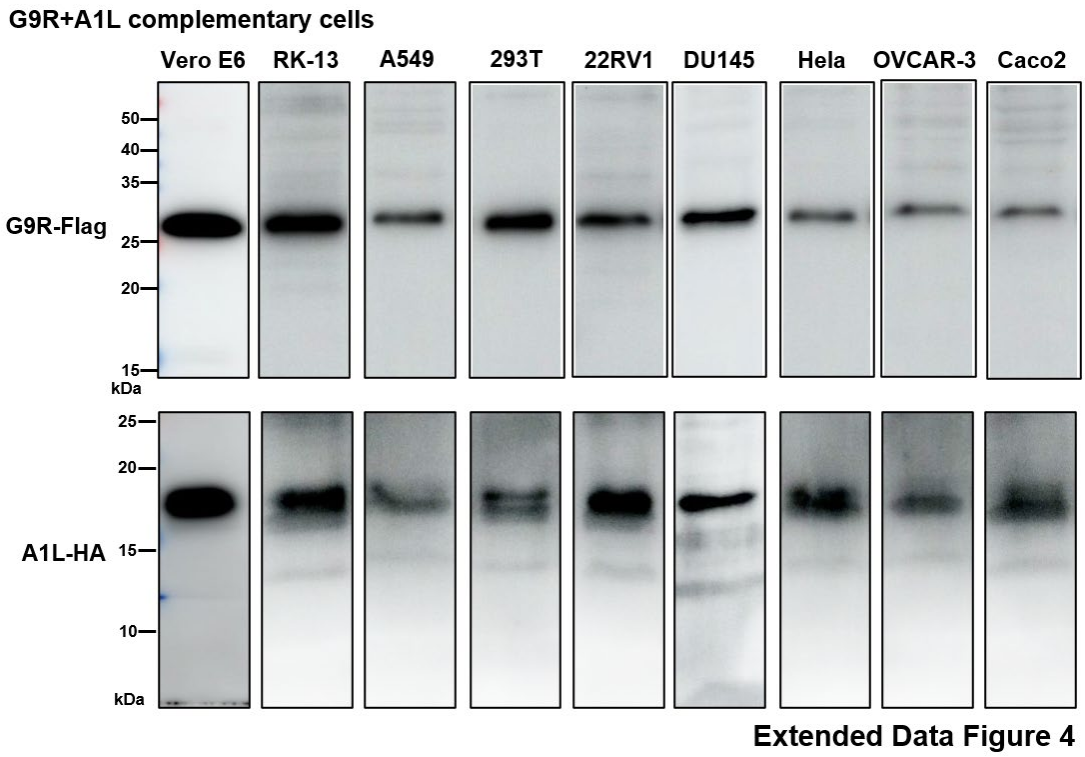

Extended Data Figure 4. The expression of G9R and A1L genes in various complementary stable cell lines.

The expression of G9R and A1L genes in 9 G9R+A1L complementing cells were detected by western blot. The G9R and A1L proteins were respectively fused with flag or HA tags at the N-terminal of the proteins. For different types of cells, the cell numbers for the blotting are normalized to an equal amount.

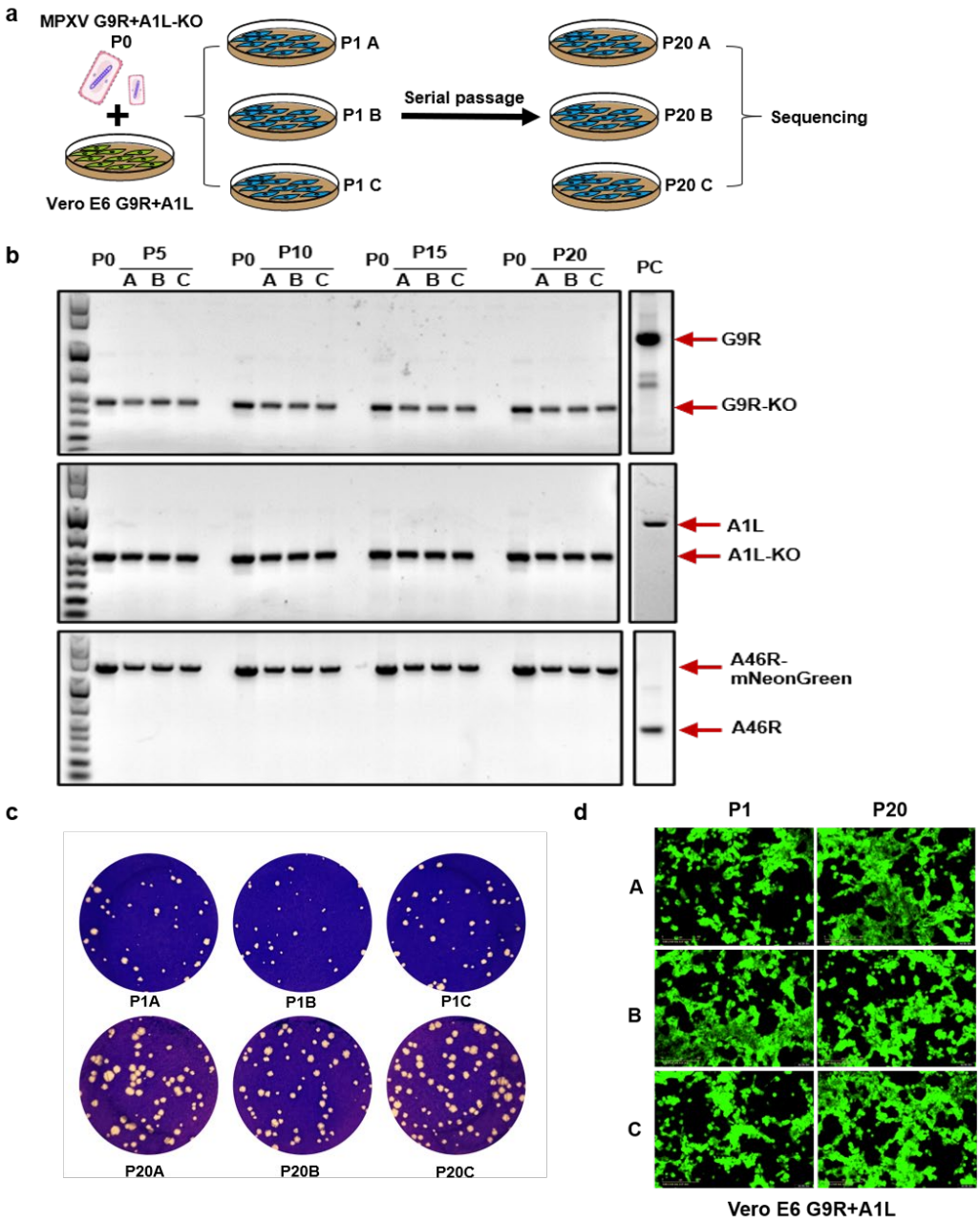

Extended Data Figure 5

Extended Data Figure 5. The serial passage of deficient MPXV in Vero E6 complementing cells.

a, Experimental scheme of serial passage of deficient MPXV in Vero E6 G9R+A1L cells. MPXV G9R+A1L-KO virion was continuously passaged on Vero E6 G9R+A1L cells for 20 rounds in 3 replicates. The full-length MPXV genome of P0 and P20 were subjected to sequencing. **b,** PCR confirmation of G9R and A1L gene deletions and mNeonGreen insertion in MPXVs across various passages. The samples were collected at passages 5, 10, 15, and 20, with P0 initial viruses serving as controls. **c,d** The plaque morphology (**c**) of fluorescence (**d**) comparison of deficient MPXV after serial passages. **c,** The plaques of MPXV G9R+A1L-KO virus at passage 1 and passage 20 in Vero E6 G9R+A1L cells were stained with crystal violet 6 days post-

791 infection. **d,** Vero E6 G9R+A1L cells were infected with P1 and P20 MPXV deficient
792 viruses at MOI of 0.1. Representative mNeonGreen positive images are shown 4 days
793 post-infection. Scale bar, 200 μm.

794

795 **Extended Data Table 1. The detected mutations of deficient MPXV after 20**
796 **passages.**

No.	Genome region*	Product	Nucleotide	Amino acids	Replication
1	ITR	Noncoding Region	^627T	N/A	A,C
2	MPXVgp016	D13L	G18318A	silent mutation	A
3	MPXVgp076	G7R	C71481T	S32L	C
4	MPXVgp087	L3R	C79608T	silent mutation	A,C
5	Between MPXVgp125 and gp126	A15.5L	^121859T	Encode differently after K29	A
6	MPXVgp149	A39R	Δ143739C	frame shift	B
7	MPXVgp149	A39R	T143761G	L79R	C
8	MPXVgp149	A39R	G144060T	D179Y	A
9	MPXVgp150	A40L	G145081T	Q113K	A
10	MPXVgp151	A41L	C146786A	frame shift	A,C
11	Between MPXVgp151 and gp152	Noncoding Region	Δ146878-146922	N/A	A,B,C
12	MPXVgp152	A42R	Δ146999T	frame shift	A,B,C
13	Between MPXVgp172 and gp173	Noncoding Region	T170970G	N/A	A,B,C
14	Between MPXVgp179 and gp180	Noncoding Region	Δ179151-179204	N/A	A,B,C
15	ITR	Noncoding Region	^196594T	N/A	A,C

797 The mutations in the noncoding and coding regions of MPXV G9R+A1L-KO between
798 passages P0 and P20 are noted. * symbol means the region of MPXV MA001 genome
799 (ON563414.3), ^ symbol means insertion, Δ symbol means deletion. A or B or C is
800 biological replicate; N/A, Not Applicable. Sequences have been deposited to figshare
801 website (Licence ID: CC BY 4.0, DOI: 10.6084/m9.figshare.26340355).

802 **Extended Data Table 2. The IC_{50} values derived from plaque formation assay**
803 **and mNeonGreen positive cell counting assay.**

Drugs	Cells	IC_{50} uM (PFU)	IC_{50} uM (Fluorescence)
Tecovirimat	Vero E6 G9R+A1L	0.0038	0.002215
Cidofovir	Vero E6 G9R+A1L	6.776	1.239
Raltitrexed	A549 G9R+A1L	0.0823	0.2542
Tecovirimat	A549 G9R+A1L	0.0652	0.01138
Cidofovir	A549 G9R+A1L	48.29	12.83
Brequinar	A549 G9R+A1L	0.1236	0.4039
Buparvaquone	A549 G9R+A1L	3.854	5.956
Narasin	A549 G9R+A1L	0.0583	0.1294

804

805 **Extended Data Table 3. Primers used for construction of deficient MPXV.**

MPXV-F1	Forward primer	Reverse primer
F1a	GGAGTCACTAGTATTTAGGTGACACTATAGAAGGCG CGCCATACACCTGCAAAATGTGTGACCCACGACCGT AGGAAACT	AATAATCTATATGATTGGAGAAGTAGGAAACAAA CAGTAACAAGACGACG
F1b	ATCGTCGTCTTGTTACTGTTTGTTTCCTACTTCTCCA ATCATATAGATTATT	AATAATATAAGGATGATGAGAGGACGAGGATAGA TCGAAAAAAGCCACTA
F1c	ATTAGTGGCTTTTTTCGATCTATCCTCGTCCTCTCAT CATCCTTATATTATT	ATCGAATTCCATATCCGCGACTAAACAGTGAAAA ATGTAAATACTTTTTAAAT
F1d	TTTAAAAAGTATTTACATTTTTCACTGTTTAGTCGCGG ATATGGAATTCGATCCTG	TGTGCGGGTGTATAGAGTTCACAGTAGCTCATTC ACTTCTATTCAGTCAAAATG
F1e	TTTTGACTGAATAGAAGTGAATGAGCTACTGTGAACT CTATACACCCGCACAACTA	ATGAGTCCATGGATTAATATGAGTATAGTGTTAAA TGACACTTACTAAAAGCCAAA
F1f	GCTTTTAGTAAGTGTCATTTAACACTATACTCATATTA ATCCATGGACTCATAATC	GTATAAACTATCACGCGTTTGAATCGATATTAGAC TATATGCGCTGGAAGAAGATA
F1g	TTCTTCCAGCGCATATAGTCTAATATCGATTCAAACG CGTGATAGTTTATACCATT	TATTAATTTTTATACTATAATGGACAACACAACATT ATGTCGGTCGAGTATTATCT
F1h	AATACTCGACCGACATAATGTTGTGTTGTCCATTATA GTATAAAAATTAATATTTC	GTTAAGAGATGCATATGGATAGATATGTTGAATAT AGGGATAAACTTGTAGGGAAA
F1i	CCTACAAGTTTATCCCTATATTCAACATATCTATCCATA TGCATCTCTTAACACTC	TTTAAATTAATACGACTCACTATAGGGTCAGTGC GGCCGCCACCTGCTAATAGAATGCTAACGTAATA ATGCGTTATGAA
MPXV-F2	**Forward primer**	**Reverse primer**
F2a	GGAGTCACTAGTATTTAGGTGACACTATAGAAGGCG CGCCCACCTGCAGCATTCTATTATCCAGTGTTAAAAA AATTATC	TAACTGAAAAAAAATTACTACTATTGTTAATTTAGT TATGGAACCTATCCTTGCAC
F2b	AAGGATAGGTTCCATAACTAAATTAACAATAGTAGTAA TTTTTTTTCAGTTATC	ACCTGGACTTTCGTTTGTAAATTGGGGCTTTTTG TACAATAAATGGGTGTTGCC
F2c	CAACACCCATTTATTGTACAAAAAGCCCCAATTTACA AACGAAAGTCCAGGTTTGAT	TAGAAAATAGAGACGTTATAGAACGCCATCATGT TAAACAGGATACAAACCTTGATG
F2d	AGGTTTGTATCCTGTTTAACATGATGGCGTTCTATAA CGTCTCTATTTTCTATTTT	TACAAAATGAGAATTCATTTATAGCATAGAAAAAA ACAAAATGAAATTCTACTATA
F2e	GTAGAATTTCATTTTGTTTTTTTCTATGCTATAAATGAA TTCTCATTTTGTATCCGC	ACAAATTTTAGTACTATTAACGCGACTAGTATTCT CTAAAGATGATATCTGT
F2f	ACAGATATCATCTTTAGAGAATACTAGTCGCGTTAATA GTACTAAAATTTGTAT	ATATACAAATTATTAATAATATATTTGGTTTGTTCTA TGATCTACCGTGCCTTATC
F2g	AGGCACGGTAGATCATAGAACAAACCAAATATATTAT TAATAATTTGTATATACAT	TTTAAATGAAAATATATTTCTAAATTCTAGAAATGG ATGTTAGGTGTATTAATTGG
F2h	TTAATACACCTAACATCCATTTCTAGAATTTAGAAATAT ATTTTCATTTAAATGAATC	TTTAAATTAATACGACTCACTATAGGGTCAGTGC GGCCGCCACCTGCTATAGCGTTTGTCTTCTGTA GTTGGTTATCATA
MPXV-F3-G9R-KO-mCherry	**Forward primer**	**Reverse primer**
F3a	GGAGTCACTAGTATTTAGGTGACACTATAGAAGGCG CGCCCACCTGCACAAACGCTATAAAAAACATAATTAC GACGAGC	TAAATAATTTTTTTTATTACACCAACAAAAATGTTT GTCATTAAACGAAATGGATA
F3b	CATTTCGTTTAATGACAAACATTTTTGTTGGTGTAATA AAAAAAATTATTTAATTTTTCA	AAAAGATGTGGTCATTAGATTTTGATTTTTAGTTA TTATCTACAGGAACAAATATAGTAT
F3c	TTTGTTCCTGTAGATAATAACTAAAAATCAAAATCTAA TGACCACATCTTTTTTTAGA	ACGATTTTAAGTTTTTGATACCCATAAATGAAGAA CGTACTGATTATTTTCGGTAAAC
F3d-G9R-KO-mCherry	CGAAAATAATCAGTACGTTCTTCATTTATGGGTATCAA AAACTTAAAATCGTTACT	ACTTACTCCGCCACCCATATTTATCTCATTGAAA GTATTAGTCTAAAAACGCCATA
F3e	GCGTTTTTAGACTAATACTTTCAATGAGATAAATATGG GTGGCGGAGTAAGTGTTG	TACATTAGGAACATTCTCCATTTATAGTAATCAAT CCTTTGTCGGAATATCTGTTA
F3f	AGATATTCCGACAAAGGATTGATTACTATAAATGGAG AATGTTCCTAATGTATACT	GAGATTACAGCCATTTTTATCAAGTCAGTTTCTTT TAAAGAACCGAAGGTATACAA
F3g	ATACCTTCGGTTCTTTAAAAGAAACTGACTTGATAAA AATGGCTGTAATCTCTAAG	TTTAAATTAATACGACTCACTATAGGGTCAGTGC GGCCGCCACCTGCTCTAACACTTATTCCATATTA CTAAGATCGGAA
MPXV-F4-A1L-KO	**Forward primer**	**Reverse primer**
F4a	GGAGTCACTAGTATTTAGGTGACACTATAGAAGGCG CGCCCACCTGCATAAGTGTTAGATAAATGCGGTAAC AAATGTTC	TTCGTAATTGACCACGCCATTACGATACAAACTT AACGGATATCGCGATAATGAAA
F4b	ATTATCGCGATATCCGTTAAGTTTGTATCGTAATGGC GTGGTCAATTACGAATAAAGC	ATGATACTATGTTGGCATCCATATTGTGTTTTATTA TAAACGACTAGTTTTTTTTC

F4c	AAAAACTAGTCGTTTATAATAAAACACAATATGGATGCCAACATAGTATCATCTT	ATAGCCGCATCCATTTAGAACACAAGTTAAAATTTCACTAAAGCATTAATAAATAA
F4d	TTATTAATGCTTTAGTGAAATTTTAACTTGTGTTCTAAATGGATGCGGCTATTAGAGG	ACAAAGCTCGACATTTATTTCTTTATATATCTCATCAGTTTTATGGAGAAGATACCAC
F4e	TCTTCTCCATAAAACTGATGAGATATATAAAGAAATAAATGTCGAGCTTTGTTACC	TTTTTAAAACATAGTTATTACTTATCACTCATAAATGAGTAAATCACACGCGGCCT
F4f-A1L-KO	CGCGTGTGATTTACTCATTTATGAGTGATAAGTAATAACTATGTTTTAAAAATCAC	CTTGTTCATTAGAAGTATAAAAGACGGTGTTTACGGAAGCT
F4g	AGCTTCCGTAAACACCGTCTTTTATACTTCTAATGAACAAG	TAATAAGATTGGATATTAAAATCACGCTTTCGAGTAAAAACTACGAATATAAATAA
F4h	TTATATTCGTAGTTTTTACTCGAAAGCGTGATTTTAATATCCAATCTTATTACTTTTG	TTTAAATTAATACGACTCACTATAGGGTCAGTGCGGCCGCCACCTGCTAAATCTGTAAATAAATAATGGACAAACTTAGA
MPXV-F5	**Forward primer**	**Reverse primer**
F5a	GGAGTCACTAGTATTTAGGTGACACTATAGAAGGCGCGCCCACCTGCTTTACAGATTTAGTTGTTTAATTTATTTGTGCT	TGACTCTGTCTCTTTTGATGATGAATAAATGTCATGTTATACAGCTATATTAAAATC
F5b	TAATATAGCTGTATAACATGACATTTATTCATCATCAAAAGAGACAGAGTCACCAT	TTGTCTGGATATGGGAATGTATTAAATTAAATAATTTTAATTCGTTTAACGAATATCT
F5c	TCGTTAAACGAATTAAAATTATTTAATTTAATACATTCCCATATCCAGACAACAATCG	ATACTCCATCTTTAATAGTGACATTTTTTAATATATAAATGAGTTATTTAAGATAT
F5d	CTTAAATAACTCATTTATATATTAAAAAATGTCACTATTAAAGATGGAGTATAATCT	TTTAAAATAGTCGAAATGGCGTTACTAACGTTATTACATTTTTTTTATGTAATTTCT
F5e	TTACATAAAAAAAATGTAATAACGTTAGTAACGCCATTATGGATAATCTATTTACCTT	AGTGAATTAGCTTATCTTGATGAGTATCTACTAAACAATATTATACCAGAAAAGACG
F5f	TTTCTGGTATAATATTGTTTAGTAGATACTCATCAAGATAAGCTAATTCACTAAACAT	GGGAGATCTACGATCTTATAATTACCCGATTGTAGTTAAGTTTTGAATAAAAATTT
F5g	TTTTATTCAAAACTTAACTACAATCGGGTAATTATAAGATCGTAGATCTCCCATGT	CCTAAGTGTATTTAAAATAGATGTCATGTTAAAAATGTCAGCTGCCGACTTTTTGGAA
F5h	AAAGTCGGCAGCTGACATTTTTAACATGACATCTATTTTAAATACACTTAGGTTTT	TTTAAATTAATACGACTCACTATAGGGTCAGTGCGGCCGCCACCTGCACGTTAACGACTTACTATTAATTCATTTTTTGT
MPXV-F6-A46R-mNG	**Forward primer**	**Reverse primer**
F6a	GGAGTCACTAGTATTTAGGTGACACTATAGAAGGCGCGCCCACCTGCAGTCGTTAACGTACGCCGCCATGGACGCCGCGT	AAGAAAAAAATTGATAATTGTTAATTGTTATTTTTATACAACAAAACGGTACGGTG
F6b	GTACCGTTTTGTTGTATAAAAATAACAATTAACAATTATCAATTTTTTTCTTTAATAT	CTTCTCCTTTGCTCACCATTATTTAGTAAAATAGAAT
F6c-mNeonGreen-F2A-A46R	ATTCTATTTTACTAAATAATGGTGAGCAAAGGAGAAG	CTCGACGTCTCCCGCCAGCTTGAGAAGGTCAAAATTCAACAGCTGCTTGTAGAGTTCGTCCATT
	GACCTTCTCAAGCTGGCGGGAGACGTCGAGTCCAACCCTGGGCCAATGGCTGTTTGTATAATAG	ACGTATCACTTGTTTAATATCTATATCAGCTATTCTGGAACCGAGTACTTCCACAT
F6d	GGAAGTACTCGGTTCCAGAATAGCTGATATAGATATTAAACAAGTGATACGTAAGA	AAAAAAATAACAAATATGGAATACAACCTTATATATTTTTGCTCTCATTAACTTTT
F6e	GTTAATGAGAGCAAAAATATATAAGGTTGTATTCCATATTTGTTATTTTTTTCTGT	CCTCTCAATATGATAGATTTTATTATCCCAGATATTTATGTAAGTCAAAAATCTAG
F6f	ATTTTTGACTTACATAAATATCTGGGATAATAAAATCTATCATATTGAGAGGACCA	TATATAATTTATATTCTGTAACATGTTATCCCTTTTCAATGAACAGTGTTAGTTTA
F6g	CTAACACTGTTCATTGAAAAGGGATAACATGTTACAGAATATAAATTATATATGGA	CATGGTGTTGTTTGTTATTTGACTACTGTCACTGAAGTGATAATATATTTTAAATTTT
F6h	TAAAATATATTATCACTTCAGTGACAGTAGTCAAATAACAAACAACACCATGAGAT	TTTAAATTAATACGACTCACTATAGGGTCAGTGCGGCCGCATTGGTCGTGTAGCGCGATAGAGATAGTCTAATAT
MPXV-F7	**Forward primer**	**Reverse primer**
F7a	GGAGTCACTAGTATTTAGGTGACACTATAGAAGGCGCGCCCACCTGCACACGACCAATATCGATTACTATGGATATCTTC	TCTTCATCTTCATCTTCATCTTCATCATAGGTACTAAGATAATTATATAATATCAGTT
F7b	TATTATATAATTATCTTAGTACCTATGATGAAGATGAAGATGAAGATGAAGATGATGG	TAACATCTTCTACTTATCATCACCCATTGTATAACATTCTATAGTTCGTTTTACGTTC（
F7c	AAAACGAACTATAGAATGTTATACAATGGGTGATGATAAGTAGAAGATGTTACCCGAT	TCCAAAAATCCTATATTACCATGTAATGTGTTATTGTTAGATGTCTCATCATCAAC
F7d	ATGATGAGACATCTAACAATAACACATTACATGGTAATATAGGATTTTTGGAAATAAA	TATGTCCGTTTCTTAGTTTTAGCATCTTCCCAAAATGAATTAGGGTTGTCATATCCAT
F7e	ATGACAACCCTAATTCATTTTGGGAAGATGCTAAAACTAAGAAACGGACATATAGTGC	TCTTAGAAATGCCATTCGTATGTACACGCTGGCAGACGCCACCGAGCTGTCATAGT

F7f	TGACAGCTCGGTGGCGTCTGCCAGCGTGTACATAC GAATGGCATTTCTAAGAAAAG	GGCTTTTTTCGATCTATCAATTTCAGTATATTCGT CGCCGTTATAAAAGTAATGTTGT
F7g	TTACTTTTATAACGGCGACGAATATACTGAAATTGATA GATCGAAAAAAGCCACTAAT	CTATCTTATCGAATGATATATTTTTCATAAATACAC TTTTATAGTCCTCGTTTAAACA
F7h	AAAAGTGTATTTATGAAAAATATATCATTCGATAAGATA GATTCCATCATCGAAAAAT	TTTAAATTAATACGACTCACTATAGGGTCAGTGC GGCCGCATACACCTGCAAAATGTGTGACCCACG ACCGTAGGAAACT

806